



Aqueous phase reforming of starch wastewater over Pt and Pt-based bimetallic catalysts for green hydrogen production

Adriana S. Oliveira^{a,b,*}, José A. Baeza^a, Luisa Calvo^a, Miguel A. Gilarranz^a

^a Department of Chemical Engineering, Universidad Autónoma de Madrid, Campus de Cantoblanco, 28049 Madrid, Spain

^b Thermochemical Process Unit, IMDEA Energy Institute., Avda. Ramón de la Sagra, 3, 28935 Móstoles, Spain

ARTICLE INFO

Keywords:

Starch wastewater
Aqueous phase reforming
Green hydrogen
Pt-based catalyst

ABSTRACT

This work analyses the application of aqueous phase reforming (APR) for green hydrogen production from starch industry wastewater. This work reports for the first time on the direct conversion of a high molecular weight biomass polymer contained in wastewater in contrast to low molecular weight substrates mainly reported in the literature. The potential of this type of feedstock was evaluated by varying the starch source (rice, potato, sweet potato and cassava) and the type of catalyst (carbon supported Pt, PtRu, PtPd, PtRe and PtRh catalysts). In APR experiments at 220 °C with synthetic wastewater, PtRu/C and Pt/C catalysts achieved the highest H₂ yield values, around 51 mmol H₂ per g of organic carbon in the initial wastewater, close to 2.6 times higher than that reported in the literature of brewery wastewater, a promising substrate. The lack of free aldehyde or keto groups due to glycosidic bonds between glucose units in starch results in higher conversion to gas and H₂ production compared to APR of glucose. This fact shows that APR has more feedstock flexibility than that previously reported for light compounds. In the experiments with real wastewaters, the organic matter removal was influenced largely by the starch source: the best APR performance (28.5 mmol H₂ gTOC⁻¹) was obtained for rice processing wastewater, which is characterized by the highest starch concentration and the lowest protein content. Poor performance was observed in the APR of potato processing wastewater, probably due to catalyst deactivation caused by protein fraction.

1. Introduction

Environmental emergency due to global warming and concerns about energy security and access are driving worldwide a change in the sources and use of energy. Renewable energies are a central element in the transformation to cleaner and more sustainable systems. In Europe hydrogen is considered as essential to achieve net-zero emissions and sustainability targets in the framework of the region's Green Deal [1]. Thus, the production of green hydrogen, i.e., that produced using renewable raw materials and energy, is a main element in the transition to widespread use of hydrogen as feedstock, fuel and energy carrier and storage, across industry, transport, power and building sectors [2]. Accordingly, research on the production and use of green hydrogen has accelerated in the last decade. Examples of technologies proposed to produce hydrogen from renewable resources include water splitting by electrolysis, thermochemical cycles or photocatalysis [3–5]; and fermentation and thermochemical conversion of biomass [6,7]. The thermochemical routes for hydrogen production from biomass are

mainly based on gasification of biomass and reforming of the gas and bio-oil produced by biomass pyrolysis, although some approaches include supercritical water gasification and pyrolysis bio-oil gasification [8].

Aqueous-phase reforming (APR) is a thermochemical catalytic process carried out in the liquid water phase that can convert water-soluble hydrocarbons and oxygenates into hydrogen and light alkanes. APR is usually carried out at temperatures between 170 and 250 °C and pressures between 30 and 50 bar. High pressures are used to favor water gas shift reaction, although some works have reported negligible CO content in the produced even when operation slightly over water vapor pressure [9]. APR shows some interesting features related to the use of liquid water as reaction medium, such as compatibility with high water content feedstocks and reduced energy consumption, which typically high in processes requiring higher temperatures and vaporization of feedstocks [10].

The reaction mechanism in APR is highly dependent on the substrate reformed and the catalysts used, however common steps include

* Corresponding author at: Thermochemical Process Unit, IMDEA Energy Institute., Avda. Ramón de la Sagra, 3, 28935 Móstoles, Spain.

E-mail address: adriana.souzade@uam.es (A.S. Oliveira).

<https://doi.org/10.1016/j.cej.2023.141770>

Received 14 October 2022; Received in revised form 25 January 2023; Accepted 5 February 2023

Available online 9 February 2023

1385-8947/© 2023 The Author(s). Published by Elsevier B.V. This is an open access article under the CC BY-NC license (<http://creativecommons.org/licenses/by-nc/4.0/>).

dehydrogenation, cleavage of C—C, hydrodeoxygenation by cleavage of C—O bonds, methanation and water gas shift reaction [11]. A wide variety of products can be generated from C₁ to C₆ together with hydrogen.

Pt-based catalysts are among the most used in APR since they promote conversion through C—C cleavage, which enhances hydrogen production [12–14]. Catalysts based in transition metals such as Ni have been also tested, leading to high selectivity towards hydrogen, although their lack of stability under APR conditions limits their use [15]. Bimetallic combinations of Pt with Ru, Rh, Re, Co, Fe and Mo have been reported to improve selectivity and protect coke against coke deposition and poisoning [15]. Commonly reported supports include alumina, ceria, magnesia, zirconia, titanium dioxide, zeolite and carbon material [16–18].

Many substrates have been studied to assess the flexibility of the APR process. Model compounds and commodities considered include alcohols, polyols, sugars and organic acids [19,20]. Processing of wastewaters containing organic pollutants has been found to be an interesting option as makes possible valorization of waste and water treatment [9,21]. In this sense, recent works also show the combination of APR with liquefaction and hydrothermal carbonization of solid biomass waste [22,23].

A crucial aspect related to the type of feed used in APR is the contribution of substrates to catalyst deactivation [24]. High deactivation of catalysts and low selectivity to hydrogen has been observed in the APR of sugars due to their caramelization and reactions involving aldehyde and ketone groups of sugars [14,25]. Aho et al. [26] proposed the hydrogenation of wood sugars obtained by acid hydrolysis before subjecting them to APR, thus improving APR performance. Likewise, in a former work [27] it was shown that hydrogenation of maltose to maltitol as a pretreatment for APR result in lower deactivation of catalyst and higher net production of hydrogen, with extra 3 mol of H₂ produced for each mol of H₂ consumed in the pretreatment of maltose. The better results achieved were ascribed to prevailing degradation route of maltitol via hydrolysis generating sorbitol, instead of only glucose in the case of maltose. Likewise, in the APR of maltitol a much lower concentration was found for liquid phase compounds such as fructose, pyruvaldehyde, and HMF, which are known to be precursors in solid humins formation.

Basis on the results commented above, the current work explores the APR of starch and starch-rich wastewaters. Starch is formed by glucose units joined by glycosidic bonds, where there are not free aldehyde or keto groups since they are involved in the formation of the glycosidic bonds. This feature may contribute to degradation routes in APR leading to lower deactivation and higher hydrogen production. Likewise, previous exploratory work has shown that starch used to prepare model synthetic urban shows good processability in APR [28]. Starch wastewater is generated in large volumes in sugar refineries, large scale sushi production and in the industrial processing of potato and cassava, among others [29]. Therefore, there is a niche for coupling waste treatment and valorization by conversion to hydrogen by APR. Furthermore, it should be noted that the current work explores for the first time the direct conversion of a high molecular weight biomass polymer contained in wastewater in contrast to low molecular weight substrates mainly reported in the literature. To assess the potential of this type of feedstocks, synthetic and real wastewater from processing of rice, potato, sweet potato and cassava have been treated by APR using Pt and Pt-based bimetallic (PtRu, PtPd, PtRe, PtRh) catalyst supported on a carbon support. The influence of the type of catalysts, starch source and feedstock concentration have been evaluated.

2. Experimental

2.1. Materials

Hexachloroplatinic acid solution (8 wt% in H₂O), palladium (II)

chloride (99 %), ruthenium (III) chloride (45–55 %), rhodium (III) chloride (98 %), perrhenic acid solution (75–80 wt% in H₂O) and starch from potato (soluble) were purchased from Sigma-Aldrich. Commercial ENSACO 250 G carbon black was supplied by TIMCAL Canada Inc.

2.2. Preparation and characterization of support and catalysts

Mono- and bimetallic Pt, PtRu, PtPd, PtRe and PtRh catalysts were prepared by sequential incipient wetness impregnation using a carbon black (ENSACO 250 G) as support. The support was not pretreated or functionalized before metals impregnation. The nominal metal load was 3 wt% for all catalysts and the metal molar ratio for the bimetallic ones was 1:1. After impregnation, the catalysts were dried overnight at 60 °C, then they were calcined for 2 h at 200 °C in the case of monometallic Pt catalyst and 250 °C in the case of bimetallic Pt-based catalysts. Finally, they were reduced at 300 °C for 2 h under H₂ flow (25 mL N/min).

The support and prepared catalysts were characterized by N₂ adsorption–desorption isotherms at –196 °C using a TriStar II Micromeritics analyzer. The acidity of the materials was estimated from pH slurry measurements, which was determined according to the procedure describe in the literature [30]. In addition, elemental analysis of some used catalysts was performed to determine the surface CHNS-O composition using a LECO CHNS-932 elementary chemical analyzer. Scanning transmission electron microscopy (STEM) images of the catalysts were recorded with a JEOL – 3000F microscope operated at 300 kV. More than 200 metals nanoparticles were measured using the Software ‘ImageJ 1.51 k’ to obtain the size distribution histograms of the materials. The metal loads in the catalysts were determined by a Perkin-Elmer ICP-MS Nexion 300XX apparatus. X-ray diffraction (XRD) analyses of catalysts for characterization of metals on the support were carried out by a X’pert PRO Theta diffractometer, in the 10–80° range. X-ray photoelectronic spectroscopy (XPS) profiles of the catalysts were recorded using a PHI VersaProbe II instrument equipped with X-ray excitation source, Al 1486.6 eV mono at 47.8 W. Software ‘XPS peak v4.1’ was used for the deconvolution of the peaks. The data analysis procedure involved smoothing, a Shirley background subtraction and mixed Gaussian–Lorentzian by a least-square method for curve fitting. C1s peak (284.6 eV) was used as internal standard for binding energies corrections due to sample charging.

2.3. Preparation and characterization of starch wastewater

Synthetic starch wastewater (SSW) and real starch-based wastewater (RSW) were used as feedstocks for APR experiments. SSW was prepared with 1 wt% of a commercial starch, and for its complete solubilization, the aqueous mixture was heated at 90 °C, under 250 rpm stirring, for 1 h. RSW were prepared using rice, potato, sweet potato, and cassava as starch source. These raw materials were ground in water (around 3 mL of water per g of raw material) until a homogeneous aqueous slurry was obtained, which was heated for solubilization of the starch as described above for SSW. Subsequently, the resulting solution was filtered, and its concentration was adjusted to a total organic carbon (TOC) value equivalent to that of SSW.

SSW and RSW were characterized by TOC, measured in a TOC-VCSH apparatus (Shimadzu), chemical oxygen demand (COD), according to the ASTM D1252 standard method, and total nitrogen (TN), measured in a TOC-NT VCSH apparatus (Shimadzu). In addition, the soluble starch concentration of the samples was estimated by spectroscopic analysis (UV–vis, Cary 60, Agilent Technologies) and the main short chain organic acids were detected by ionic chromatography (883 Basic IC Plus, Metrohm). For UV–vis analysis, 3 mL of the sample was placed in a test tube and 1 mL of an I/KI solution (0.01 M) was added, then the intensity of the blue colour produced was measured at 610 nm against a reagent blank. Due to the high concentration of starch in the SSW and RSW, the samples were diluted before UV–vis analysis using a ratio of 1:1000. The concentration of soluble starch in the samples was calculated from a

standard curve prepared in the range of 0–50 mg of starch mL⁻¹, treated in the same manner as the test sample. Each characterization test was performed at least in duplicate, and the reported value is the average obtained (the standard deviation was <10 % in all samples).

2.4. Aqueous phase reforming experiments

The APR experiments were carried out in a batch reactor (BR100, Berghoff) at 220 °C, 26–29 bar and 500 rpm using 20 mL of wastewater and 0.4 g of catalyst. Before starting the experiments, the reactor was purged 3 times with Ar and the initial Ar pressure was adjusted to 5 bar. The reaction time was established in 4 h. After this time, the heating and stirring were stopped and the reactor was cooled down until the room temperature. Then, the gas produced was collected in multilayer foil sample bags (Supelco, USA) and it was analysed by a GC/FID/TC (7820 A, Agilent) composed by 2 packed columns and a molecular sieve. The effluents obtained after the reaction experiments were filtered and characterized as the feedstocks. All APR experiments were performed at least by duplicate.

The organic matter removal was estimated by TOC and COD removal according to Eq. (1).

$$TOC \text{ or } COD \text{ Removal}(\%) = \frac{TOC \text{ or } COD_{initial}(\frac{mg}{L}) - TOC \text{ or } COD_{final}(\frac{mg}{L})}{TOC \text{ or } COD_{initial}(\frac{mg}{L})} \times 100 \quad (1)$$

The carbon conversion to gas (CC_{gas}) was calculated according to Eq. (2), and the carbon conversion to liquid (CC_{liq}), including compounds initially present in the wastewater that have not reacted, was calculated using Eq. (3). The carbon conversion to solid (CC_{sol}) was estimated using Eq. (4).

$$CC_{gas}(\%) = \frac{C_{gas(g)}}{C_{initial(g)}} \times 100 \quad (2)$$

$$CC_{liq}(\%) = \frac{C_{liq(g)}}{C_{initial(g)}} \times 100 \quad (3)$$

$$CC_{sol}(\%) = 100 - CC_{liq}(\%) - CC_{gas}(\%) \quad (4)$$

where C_{gas} and C_{liq} are the total amounts of carbon in the gas and liquid phases after APR, respectively, and $C_{initial}$ is the amount of carbon initially present in the wastewater.

H₂ selectivity was calculated by Eq. (5), and CO₂ and alkanes selectivity (S_i) were calculated by Eq. (6).

$$Selectivity_{H_2}(\%) = \frac{H_{2,gas} \times 2(mol)}{\text{Total of hydrogen in the gas phase products}(mol)} \times 100 \quad (5)$$

$$Selectivity_{CO_2 \text{ or } alkanes}(\%) = \frac{C_{i,gas}(mol)}{C_{gas}(mol)} \times \frac{1}{R} \times 100 \quad (6)$$

where $C_{i,gas}$ is the amount of carbon detected in a product i (CO₂ or alkanes) in the gas phase.

H₂ and alkanes yield were calculated according to Eq. (7).

$$Yield_{H_2 \text{ or } alkanes}(mmol_i/g_{TOC_i}) = \frac{mmol_{H_2 \text{ or } alkanes}}{TOC_{initial(g)}} \times 100 \quad (7)$$

3. Results and discussion

3.1. Characterization of support and catalysts

Table 1 shows the textural properties, the pH slurry, and the mean sizes of metal nanoparticles (obtained from STEM images) of the support and/or catalysts. The N₂ adsorption/desorption isotherms are included as [supplementary information](#) (Fig. S1). The support yielded a BET

Table 1

Characterization of supports and catalysts.

Samples	S _{BET} (m ² g ⁻¹)	Micropore volume (cm ³ g ⁻¹)	Mesopore volume (cm ³ g ⁻¹)	pH slurry	Mean nanoparticle size (nm) ^a
Support	65	<0.001	0.09	8.9	–
Pt/C	64	<0.001	0.09	8.6	4.7 ± 2.5
PtRu/C	64	<0.001	0.09	7.5	2.3 ± 1.0
PtPd/C	64	<0.001	0.09	9.1	2.7 ± 1.0
PtRe/C	64	<0.001	0.09	5.6	1.9 ± 0.6
PtRh/C	64	<0.001	0.09	6.9	2.2 ± 0.6

^a From STEM images.

surface area (S_{BET}) of 65 m²/g and mesopore volume of 0.09 cm³ g⁻¹, without significant microporosity. Furthermore, its pH slurry was basic (8.9). The metal impregnation did not produce a significant variation of the porous texture of the support, however the pH slurry of the catalysts varied from basic (PtPd/C: 9.1 and Pt/C: 8.6), to slightly basic or neutral (PtRu/C: 7.5 and PtRh/C: 6.9) and acid (PtRe/C: 5.6). Actual metal load of the catalysts was determined by ICP-MS and reasonably agree with the nominal loading within ± 10 %. Fig. 1 shows the STEM images of the catalysts and Fig. S2 depicts the nanoparticles size distribution histogram from STEM images. Regarding nanoparticle sizes, the bimetallic catalysts showed relatively similar values for the mean size of metal nanoparticles (between 1.9 and 2.7 nm), while the mean size of the Pt/C catalyst nanoparticles was larger (4.7 nm) (Table 1).

Fig. 2 shows the XRD patterns of the catalysts synthesized. The diffraction peak near to 25° (2θ) in all catalysts patterns is attributed to the [002] graphite basal planes of the carbon support. Additionally, the less intense broad peak at around 43° (2θ), characteristic of the [10 *l*] reflection, can be observed. The peaks at 2θ values of 39.8, 46.2 and 67.5° in the Pt/C catalyst corresponds to the [111], [200] and [220] crystal planes of Pt, respectively, which are characteristic of the face centered cubic (fcc) structure. Differences in the peak intensity of Pt and Pt-based bimetallic catalysts with respect to C could be related to differences in Pt crystallite size [31]. Regarding the bimetallic catalysts, the broadening of the XRD peaks and a shift in the angle may suggest the formation of a bimetallic alloy; however, this observation may not be conclusive because broadening can result from both combination of fcc Pt with the second metal catalyst and from combination of fcc Pt and the second metal catalyst with the bimetallic alloy [32]. Furthermore, bimetallic catalysts showed diffraction patterns like that of the Pt/C catalyst, which does not support alloy formation.

3.2. Characterization of starch wastewater

Table 2 shows the initial TOC, COD, TN and starch concentration of SSW and RSW. The starch source and the name and the assigned nomenclature for each RSW are also displayed. The initial TOC value for SSW was around 4000 mg L⁻¹. As described in the Experimental section, RSW were prepared with a TOC value similar to that obtained for SSW, which also led to similar COD values, between around 8500 and 10100 mg L⁻¹, for SSW and all RSWs. However, TN and soluble starch concentration varied significantly depending on the starch source. The highest concentration of soluble starch was obtained for SSW. Among RSWs, the highest soluble starch concentration was achieved for RPW (6275 mg L⁻¹) followed by PPW (2144 mg L⁻¹), while SPW and CPW showed significantly lower starch concentration values (around 400 mg L⁻¹). The highest TN value was achieved PPW (283 mg L⁻¹), probably due to its high protein content [33], while the other RSW showed TN values between 2 and 6 times lower than PPW, being the RPW the wastewater with the lowest value (46 mg L⁻¹).

Regarding ionic chromatography, acetic, formic, malonic, oxalic, and fumaric acids were detected in very low concentrations in all feedstocks, representing <0.3 % of the initial TOC.

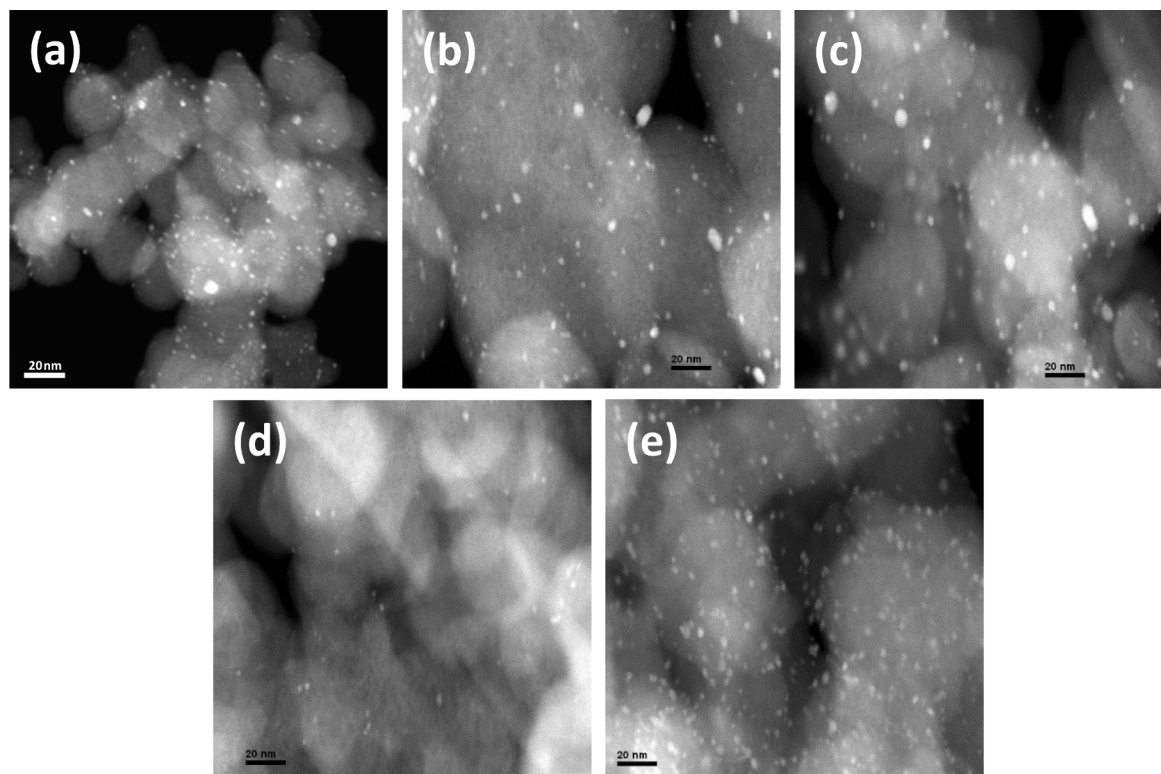


Fig. 1. STEM images of catalysts (a) Pt/C, (b) PtRu/C, (c) PtPd/C, (d) PtRe/C and (e) PtRh/C.

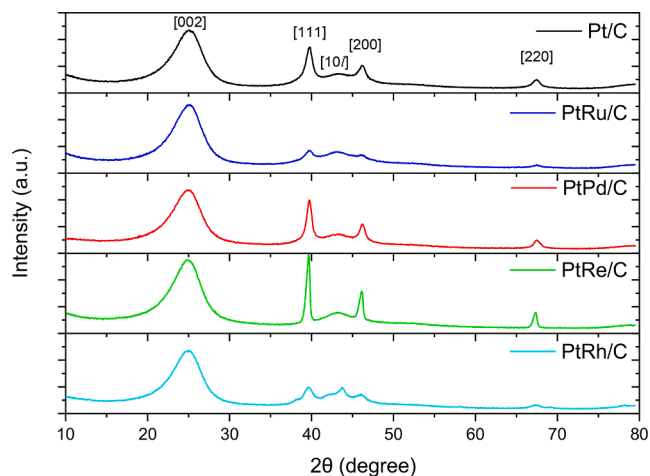


Fig. 2. XRD patterns of Pt and Pt-based bimetallic catalysts.

3.3. Aqueous phase reforming of synthetic starch wastewater

SSW was subjected to APR using mono- and bimetallic Pt, PtRu, PtPd, PtRe and PtRh catalysts to evaluate the effect of the active phase on the catalytic performance. Blank experiments (without catalyst) and with the support were also performed under the same conditions of the catalyzed experiments. Fig. 3 shows TOC and COD removal in the APR experiments with SSW. The blank test and the experiment with support showed similar TOC and COD removal values, around 55 %, which can be mostly attributed to the hydrothermal carbonization (HTC) of starch. TOC and COD removal values significantly improved in the experiments with the catalyst, up to 99.1 %, except in the case of PtRe/C, which showed removal values in a range similar to that of blanks (55.9–68.0 %). In addition, an increase in the organic matter removal was observed in presence of PtRu and PtRh catalysts in comparison to Pt, possible due to a higher catalytic activity promoted by the addition of Ru and Rh as second metals. This result is in good agreement with the work by Kaya et al. [34], which reported that the catalytic activity of Pt catalyst, in the reforming of wheat straw biomass hydrolysate, increased by 21.2 % due

Table 2
Characterization of SSW and RSW.

Feedstock	Starch source	Feedstock name	Nomenclature	TOC	COD	TN	Soluble starch concentration
				(mg L ⁻¹)			
Synthetic starch wastewater	Commercial starch	Synthetic starch wastewater	SSW	4014 ± 352	10143 ± 331	14 ± 1	9908 ± 152
Real starch-based wastewater	Rice	Rice processing wastewater	RPW	4070 ± 258	8499 ± 312	46 ± 3	6275 ± 246
	Potato	Potato processing wastewater	PPW	4092 ± 225	9790 ± 297	283 ± 22	2144 ± 192
	Sweet potato	Sweet potato processing wastewater	SPW	3840 ± 374	9702 ± 325	67 ± 18	462 ± 38
	Cassava	Cassava processing wastewater	CPW	3982 ± 388	9560 ± 310	94 ± 25	372 ± 22

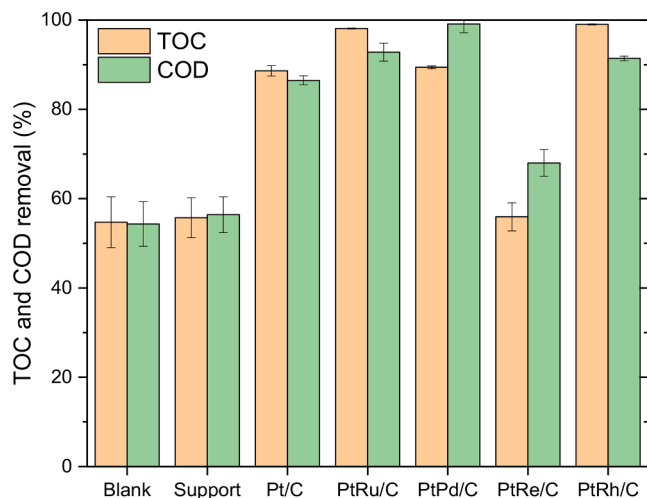


Fig. 3. TOC and COD removal in APR experiments with SSW using Pt and Pt-based bimetallic catalysts*. *Reaction conditions: 220 °C, 26–29 bar (initial Ar pressure set at 5 bar), 20 mL of wastewater, 0.4 g catalyst, 500 rpm, 4 h.

to the addition of Ru and with the study of Larimi and Khorasheh [35], which reported that the best catalytic activity in the reforming of glycerol was obtained when Rh was added to Pt catalyst. An outstanding activity in terms of conversion was reported in the APR of sorbitol using PtRe/C catalysts compared to Pt, PtNi, PtCo and PtRu catalysts [36], although this behavior was not observed in the current work.

The composition of the liquid phase after APR experiments is usually quite complex, since the reaction products are formed in a very complex network reaction, involving not only the compounds present in the feedstock but also the reaction intermediates. In addition, this network reaction is composed of several other reactions that also take place during reforming, such as dehydrogenation, decarbonylation, hydrogenation, dehydration, hydrogenolysis, HTC, polymerization, condensation, etc. As an example of this complexity, Kirilin et al. [37] demonstrated that, more than 260 compounds would be involved in the transformation of sorbitol during the APR process. In this work, some organic acids present in the liquid phase were analyzed by ionic chromatography, however, as described above, the composition of the effluent is expected to be much more complex. Therefore, future studies should be related to a thorough characterization of its composition,

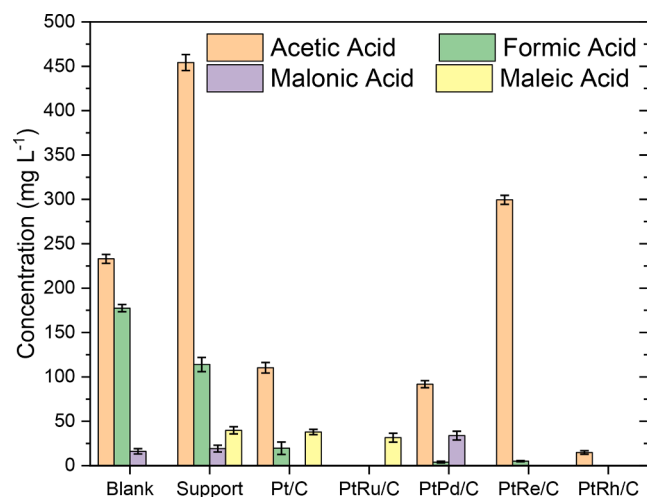


Fig. 4. Concentration of the main short chain organic acids detected after APR experiments with SSW using Pt and Pt-based bimetallic catalysts*. *Reaction conditions: 220 °C, 26–29 bar (initial Ar pressure set at 5 bar), 20 mL of wastewater, 0.4 g catalyst, 500 rpm, 4 h.

together with a specific experimental design, which can elucidate the reaction mechanism revealing the optimal pathways for H₂ production. Fig. 4 depicts the concentration of the main short chain organic acids detected after APR experiments with SSW. The concentration of these acids increased after the APR process in all the experiments, reaching 6–15 % of TOC in the treated water, a similar range to that reported previously for the APR of brewery wastewater [9]. The high concentration of acetic acid obtained in the blank experiments and in experiments with the support and PtRe/C catalyst are noticeable. In this sense, some authors [38] have reported that the acetic acid promoted the formation of coke precursors in the APR of ethylene glycol resulting in deactivation of Pt-based catalysts.

Regarding the gas products, H₂, CO₂ and alkanes were the main products detected, while CO was not observed in any of the experiments. On the other hand, in all the experiments a significant unbalance between the carbon removed from the liquid phase and the carbon detected in the gas phase was observed. As mentioned above, HTC process can also take place under APR conditions and lead to the formation of a solid phase. For this reason, CCsol was estimated from CCgas and CClq, as described in the Experimental section. Table 3 shows the gas volume produced, gas composition, CCgas, CClq and CCsol in the APR experiments with SSW. In the experiments without a catalyst (blank and support), the gas volume produced, and CCgas were very low (<6.7 mL and 3.6 %) and more than 97 % of that gas fraction was composed of CO₂, moreover the highest CCsol were obtained in these experiments (more than 50 %) confirming that HTC is the main process under these conditions. On the contrary, the percentage of CO₂ in the gas fraction was significantly lower in the catalyzed experiments, mainly for Pt, PtRu, PtPd and PtRh catalysts, which showed a percentage of CO₂ in the produced gas lower than 37.0 %. Furthermore, in the catalyzed experiments CCgas and the percentage of H₂ in the gas fraction increased compared to the experiments carried out without a catalyst. The highest gas volume, and consequently CCgas, was obtained with PtRu/C catalyst (63.0 %), however the highest percentage of H₂ in the gas fraction was obtained with Pt/C (60.2 %). The higher gas production could be attributed to a decrease in the binding energy of CO and H₂ on the catalyst surface due to the promotional effect of Ru to Pt, thus improving the performance of the catalyst [39]. Likewise, higher overall activity could be due to the combination of an increase of dehydrogenation reactions promoted by Ru and fast C—C bond cleavage activity due to Pt [40]. However, the H₂ produced is also consumed in side reactions, such as hydrogenolysis and methanation, for which Ru also shows high activity. The percentage of H₂ in the produced gas was much higher in the catalyzed experiments (more than 46.7 %) than in the blanks, except in the case of PtRe/C catalyst that reached only 16.0 % and yielded a gas fraction mainly composed by CO₂ (76.2 %). The worse reforming performance of PtRe/C could be due to the higher surface acidity of this catalyst compared to the others. The pH slurry of PtRe/C was 5.6 while the other catalysts presented values higher than 6.9. In this sense, some authors [41] have reported that acidic pH values favor the HTC of starch, which could also justify the high percentage of CO₂ in the gas for the APR experiments with PtRe/C catalyst, since CO₂ is described as the main product in the gas phase during HTC [42]. Finally, regarding alkanes production, the bimetallic catalysts showed a higher percentage of alkanes in the produced gas (between 7.9 and 16.8 %) than the monometallic Pt catalyst (6.6 %). During APR, alkanes can be formed by side reactions that consume H₂, such as methanation, Fischer-Tropsch reaction, dehydration/hydrogenation, hydrogenolysis, etc. and lower fractions of alkanes can be also formed during HTC. Therefore, this increase in alkanes production may indicate that these side reactions competing with the reforming are favored under the conditions used with the bimetallic catalysts compared to the monometallic one.

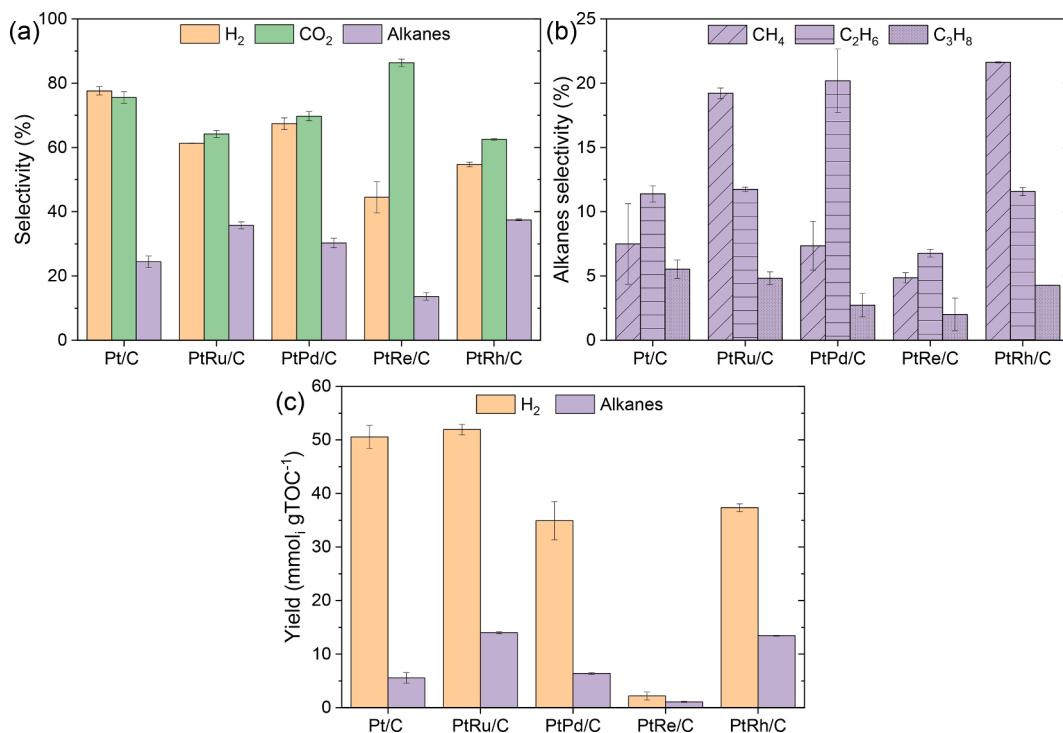
Fig. 5 shows (a) the selectivity to H₂, CO₂ and alkanes, (b) selectivity to individual alkanes and (c) H₂ and alkanes yield in the APR of SSW using Pt and Pt-based bimetallic catalysts. The selectivity to H₂ was higher for Pt/C than for the bimetallic catalysts (77.6 % versus a

Table 3

Results obtained in the APR of SSW using Pt and Pt-based bimetallic catalysts*.

Sample	Gas volume (mL)	Gas composition (% mol)					CCgas (%)	CCliq (%)	CCsol (%)
		H ₂	CO ₂	CH ₄	C ₂ H ₆	C ₃ H ₈			
Blank	6.1 ± 0.5	2.5 ± 0.6	97.2 ± 0.6	0.2 ± 0.1	0.1 ± <0.1	0.1 ± <0.1	3.3 ± 0.3	45.3 ± 5.7	51.4 ± 5.4
Support	6.7 ± 0.2	1.6 ± 0.2	98.2 ± 0.2	0.1 ± 0.1	<0.1 ± <0.1	<0.1 ± <0.1	3.6 ± 0.1	44.3 ± 4.5	52.1 ± 4.4
Pt/C	183.1 ± 5.8	60.2 ± 0.7	33.2 ± 1.6	3.3 ± 1.3	2.5 ± 0.2	0.8 ± 0.1	44.3 ± 0.3	11.4 ± 1.2	44.3 ± 0.9
PtRu/C	217.2 ± 0.5	52.1 ± 0.9	33.8 ± 1.0	10.1 ± 0.1	3.1 ± 0.1	0.8 ± 0.1	63.0 ± 0.7	1.9 ± 0.1	35.1 ± 0.8
PtPd/C	142.8 ± 6.0	53.3 ± 3.2	37.0 ± 2.5	3.9 ± 1.2	5.4 ± 0.4	0.5 ± 0.1	41.7 ± 0.2	10.6 ± 0.3	47.7 ± 0.1
PtRe/C	29.7 ± 3.4	16.0 ± 3.5	76.2 ± 3.4	4.3 ± 0.5	3.0 ± 0.1	0.6 ± 0.4	14.4 ± 1.2	44.1 ± 3.2	41.5 ± 2.0
PtRh/C	174.2 ± 1.5	46.7 ± 0.5	36.5 ± 0.3	12.6 ± 0.1	3.4 ± 0.1	0.8 ± 0.1	55.9 ± 0.2	1.0 ± 0.1	43.1 ± 0.3

*Reaction conditions: 220 °C, 26–29 bar, 20 mL of wastewater, 0.4 g catalyst, 500 rpm, 4 h.

**Fig. 5.** (a) Selectivity, (b) alkanes selectivity and (c) H₂ and alkanes yield in the APR of SSW using Pt and Pt-based bimetallic catalysts*. *Reaction conditions: 220 °C, 26–29 bar (initial Ar pressure set at 5 bar), 20 mL of wastewater, 0.4 g catalyst, 500 rpm, 4 h.

maximum of 67.4 % with PtPd/C). Regarding the selectivity to individual alkanes, APR of SSW was mainly selective to CH₄ when PtRu and PtRh catalysts were used, reaching up to 21.6 % for PtRh/C, and it was significantly lower for the other catalysts, with a minimum of 7.5 % for Pt/C (Fig. 5 (b)). Interestingly, PtPd/C catalyst was mainly selective to C₂H₆ (20.2 %), indicating different degradation routes depending on the metal active phase. Davda et al. [43] reported that Rh and Ru supported on silica favored selectivity to alkanes compared to Pt, in the APR of ethylene glycol, due to their higher catalytic activity for methanation reaction, which could justify the higher selectivity to CH₄ observed with active phases containing these metals. In addition to this, D'Angelo et al. [44] also reported that sorbitol was fully converted to CH₄ as a result of hydrogenolysis over Ru and in situ H₂ production through aqueous-phase reforming over Pt.

The specific role of Pd as a second metal in the APR of polyols with PtPd catalysts has not been reported in the literature, however the results obtained in the current work indicate that the composition of the feedstock can significantly affect the selectivity towards the different products when using this type of catalyst. Thus, He et al. [17] reported higher H₂ and CH₄ selectivity for PtPd catalyst than for Pt in the APR of glycerol, but this behavior was not observed in the APR of SSW.

As shown in Fig. 5(a) and (c), although PtRu/C had a significantly

lower selectivity to H₂ than the Pt/C catalyst (61.3 versus 77.6 %), the H₂ yield values were very similar with these two catalysts, around 51 mmol H₂ gTOC_i⁻¹, due to the higher carbon conversion and gas production for Pt/C catalyst. The alkanes yield was also similar using PtRu/C and PtRh/C catalysts, around 14 mmol alkanes gTOC_i⁻¹, while the PtRe/C catalyst yielded the lowest H₂ and alkanes yield values of all the catalysts, 2.2 and 1.1 mmol gTOC_i⁻¹, respectively (Fig. 5(c)). He et al. [17] reported a higher gas production (more than double) and an increased in H₂ yield, from 1.83 to 5.44 mmol H₂ g glycerol⁻¹ (equivalent to 4.8 and 13.9 mmol H₂ gTOC_i⁻¹), adding Ru to Pt/C catalyst. Comparing the H₂ yield obtained using PtRu catalyst with the work of He and co-workers [17], a significantly higher H₂ yield was observed when starch was used as feedstock instead of glycerol, possibly due to the lower initial concentration used for starch in the current work (1 versus 10 %), since the reaction conditions were similar (230 °C, 30 bar, 4 h).

Fig. 6 shows deconvoluted XPS spectra of the most (Pt/C and PtRu/C) and least (PtRe/C) active catalysts for the Pt 4f, Ru 3p and Re 4f region spectra. Pt bimetallic catalysts showed a higher contribution of Pt⁰ species compared to Pt monometallic catalyst (Pt⁰/Ptⁿ⁺ = 1.1–1.2 in PtRu/C and PtRe/C versus Pt⁰/Ptⁿ⁺ = 0.4 in Pt/C), evidencing that the role of Pt oxidation state has no crucial effect in the catalytic activity.

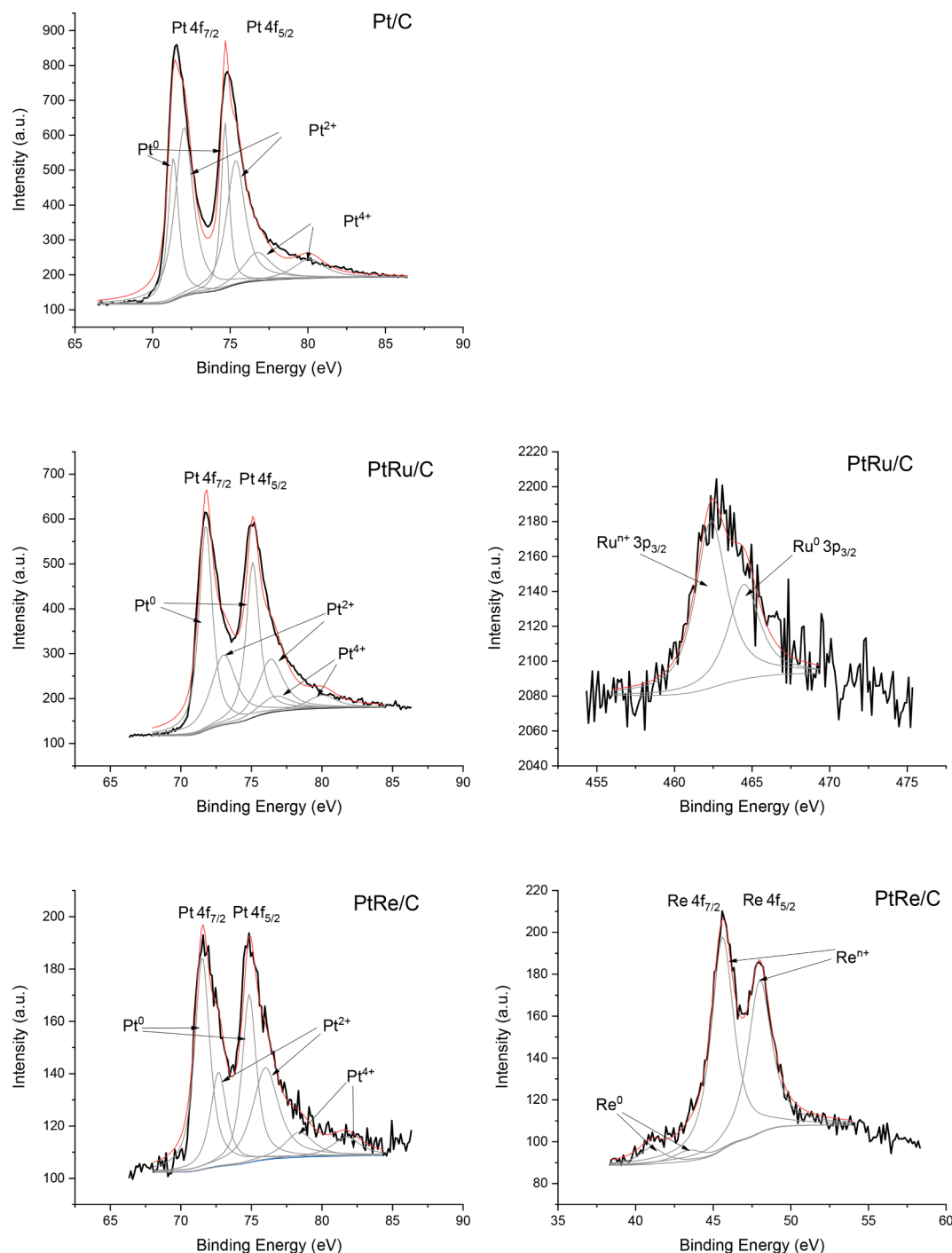


Fig. 6. Deconvolution of Pt 4f, Ru 3p and Re 4f spectra region.

Regarding the second metal, Ru^0 was prevalent ($\text{Ru}^0/\text{Ru}^{n+} = 1.8$) in the PtRu/C catalyst, whereas Re^{n+} species were clearly dominant ($\text{Re}^0/\text{Re}^{n+} = 0.1$) in the case of PtRe/C. According to the literature [45], Re favors WGS activity through facilitation of water dissociation, establishing re-OH strong bindings when used in bimetallic PtRe-based catalysts in APR. These acidic re-OH sites also increased the C—O cleavage rate in catalysts with high contribution of Re^0 in the fresh catalyst [46]. In our work, the high contribution of Re^{n+} species in the fresh catalysts could probably affect to the promoting role of Re.

3.4. Aqueous phase reforming of real starch-based wastewater

In the APR experiments with SSW, the monometallic Pt catalyst achieved high H_2 yield along with the highest H_2 selectivity among all the catalysts tested. Therefore, to maximize H_2 production, the APR experiments of RSW were carried out only with Pt/C catalyst. Fig. 7 (a) shows the values of TOC and COD removal in the APR experiments carried out with RSW, together with results with SSW as a means of comparison. A significant influence of starch source can be observed in the organic matter removal, since despite having similar initial TOC and COD concentration, RPW, SPW and CPW achieved high removal values comparable to SSW, between 70.9 and 85.4 %, while the removal values

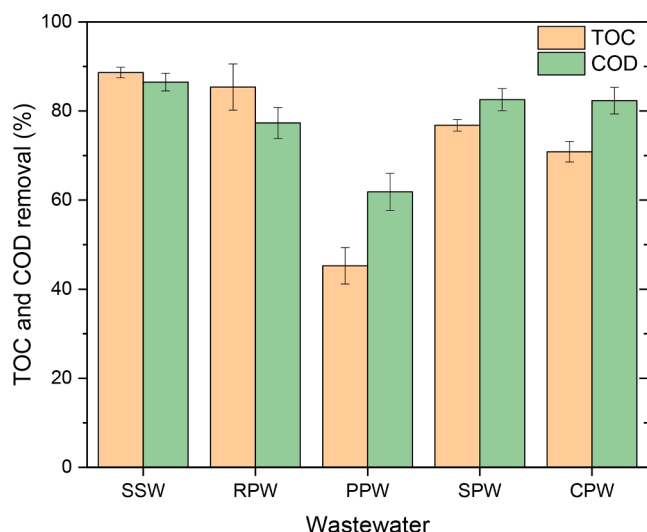


Fig. 7. (a) TOC and COD removal in the APR of SSW and RSW*. *Reaction conditions: 220 °C, 26–29 bar (initial Ar pressure set at 5 bar), 20 mL of wastewater, 0.4 g of Pt/C catalyst, 500 rpm, 4 h.

were significantly lower with PPW (45.3–61.8 %). On the contrary, although the TOC and COD removal values were different depending on starch source, the starch conversion was high, between 99 and 100 %, in all the experiments.

The concentration of the main short chain organic acids detected after APR experiments with SSW and RSW is shown in the Fig. 8. The amount of acids detected corresponded to 11–17 % of the TOC in the treated RSW, similar to 13 % detected after the APR of SSW, being acetic acid the main compound detected after APR of all RSWs. In the case of PPW the concentration of acetic acid reached almost 400 mg L⁻¹, and interestingly a very high concentration of malonic acid was also observed (249 mg L⁻¹) while this compound was not detected for SSW, RPW and SPW.

Table 4 shows the gas volume produced, gas composition, CCgas, CClq and CCsol in the APR experiments with SSW and RSW. As in the APR experiments with SSW, no CO was detected in the APR experiments with RSW. A superior APR performance was obtained with SSW, in terms of gas volume produced and percentage of H₂ in the gas fraction, however the highest CCgas was achieved with RPW (49.3 %). Among

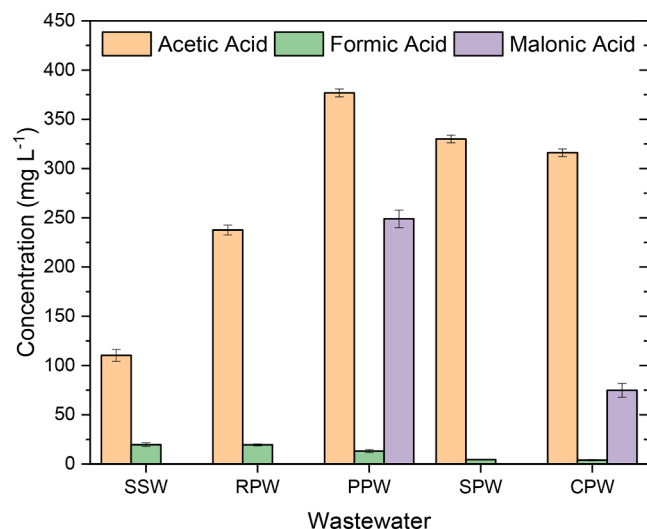


Fig. 8. Concentration of the main short chain organic acids detected after APR of SSW and RSW*. *Reaction conditions: 220 °C, 26–29 bar (initial Ar pressure set at 5 bar), 20 mL of wastewater, 0.4 g catalyst, 500 rpm, 4 h.

RSWs, the best performance was also achieved with RPW: 122.7 mL of gas with 45.4 % of H₂. This behavior can be partially ascribed to the fact that RPW contained the highest starch concentration (6275 mg L⁻¹). Thus, the RPW with lower starch concentration values, i.e. SPW and CPW (around 400 mg L⁻¹), exhibited lower performance, with similar values of gas volume and composition, CCgas, CClq and CCsol, indicating a direct correlation between the initial starch concentration and a better performance. However, PPW showed a high initial concentration of starch (2144 mg L⁻¹), but the APR experiments with this feedstock achieved a poor performance compared with the others RSW, exhibiting the lowest values of CCgas and percentage of H₂ in the gas fraction (17.2 and 35.4 %, respectively) and the highest values of CClq (54.7 %). The results with PPW could be due to its high protein content, as shown by its high TN value, which could have affected to the performance of the catalyst. In this sense, the elemental analysis (Table S1) revealed that the N and S content in the Pt/C catalyst used with PPW were around four higher than that shown by Pt/C catalyst used SSW and RPW. This is in agreement with results reported by Soták et al. [47], who observed that the Pt/C catalyst was strongly deactivated by N and S containing compounds in the APR of cellulose, losing up to 96 % of the initial activity. In this work, the loss of activity due to protein content could also be evidenced from the high concentration of malonic acid in the treated water (Fig. 8), as this organic acid is easily degraded upon APR with Pt/C catalyst [48].

Fig. 9 shows (a) the selectivity to H₂, CO₂ and alkanes, (b) a detailed selectivity of the identified alkanes and (c) the H₂ and alkanes yield in the APR experiments with SSW and RSW. The selectivity to H₂ was similar with all the RSW, between 46.7 and 56.3 %, however it was significantly higher using SSW (77.6 %). The selectivity to alkanes and CO₂ was also similar with all RSW, around 37 and 63 %, respectively, except with PPW which showed a lower selectivity to alkanes (22.5 %) and higher selectivity to CO₂ (77.5 %) (Fig. 9 (a)). Again, the high production of CO₂ could be related to lower catalytic activity and higher contribution of competing HTC.

Regarding the selectivity to alkanes, the distribution among the identified alkanes changed depending on the feedstock as can be seen in the Fig. 9(b). PPW was more selective for CH₄ production than the other alkanes, while RPW was more selective for C₂H₆ and C₃H₈ production. Finally, the results in Fig. 9 (c) show that the yield to H₂ obtained with RSW is significantly lower than that obtained with SSW. Specifically, the highest yield of H₂ achieved with a RSW (28.5 mmol H₂ gTOC_i⁻¹ with RPW) was 44 % lower than with SSW, showing the effect of minor compounds. The yield to H₂ achieved with PPW (7.5 mmol H₂ gTOC_i⁻¹) was significantly lower than with the others RSW, while SPW and CPW achieved a similar yield (17.3–21.9 mmol H₂ gTOC_i⁻¹). Therefore, the yield to H₂ was higher at higher initial starch concentration, except in the case of PPW, which despite having a high initial starch concentration achieved the lowest yield values, possibly due to its high protein content. Therefore, these results indicate that not only a high starch concentration in the wastewater is important to achieve a high yield of H₂, but also a lower content of other compounds, such as proteins, and that catalytic activity is affected by these compounds even if their concentration is low.

Comparing the results obtained in the current work with the previous results of the APR of other types of wastewaters, such as brewery wastewater, a great potential of starch-based wastewater to produce H₂ through APR is observed. Since the yield of H₂ achieved in this work with the starch wastewater was more than double that obtained with the brewery wastewater (50.5 versus 19.8 mmol H₂ gTOC_i⁻¹), at the same initial organic matter concentration and similar reaction conditions (around 4000 mg L⁻¹ TOC, 220–225 °C, Pt/C catalyst (0.02 g of catalyst per mL of wastewater)) [9].

3.5. Evaluation of catalyst deactivation

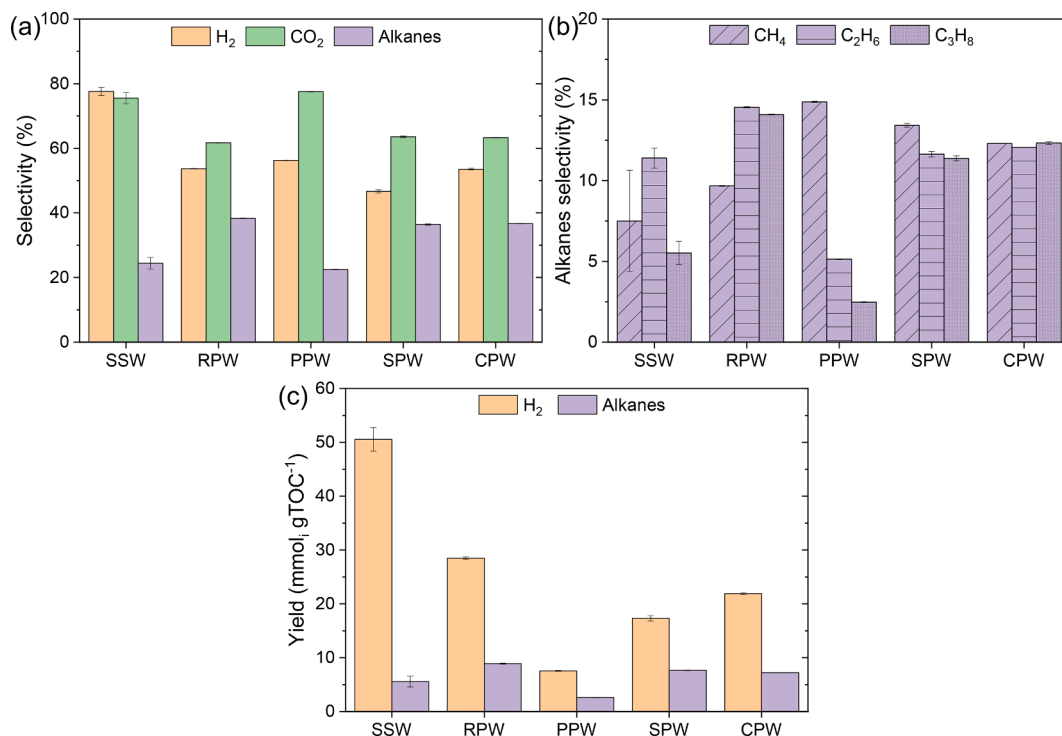
The results above indicate that the high TN value of PPW, related to

Table 4

Results obtained in the APR of SSW and RSW*.

Sample	Gas volume (mL)	Gas composition (% mol)					CCgas (%)	CCliq (%)	CCsol (%)
		H ₂	CO ₂	CH ₄	C ₂ H ₆	C ₃ H ₈			
SSW	183.1 ± 5.8	60.2 ± 0.7	33.2 ± 1.6	3.3 ± 1.3	2.5 ± 0.2	0.8 ± 0.1	44.3 ± 0.3	11.4 ± 1.2	44.3 ± 0.9
RPW	122.7 ± 1.0	45.4 ± 0.1	40.4 ± 0.1	6.3 ± 0.1	4.8 ± 0.1	3.1 ± 0.1	49.3 ± 0.4	14.6 ± 5.2	36.1 ± 4.8
PPW	41.9 ± 0.4	35.4 ± 0.1	52.3 ± 0.1	10.0 ± 0.1	1.7 ± 0.1	0.6 ± 0.1	17.2 ± 0.2	54.7 ± 4.1	28.0 ± 3.9
SPW	78.5 ± 1.1	37.5 ± 0.6	45.8 ± 0.5	9.7 ± 0.5	4.2 ± 0.2	2.7 ± 0.1	39.9 ± 0.2	23.2 ± 1.3	36.9 ± 1.1
CPW	87.6 ± 0.4	44.3 ± 0.2	41.2 ± 0.1	8.0 ± 0.1	3.9 ± 0.1	2.7 ± 0.1	38.6 ± 0.1	29.1 ± 2.3	32.3 ± 2.2

*Reaction conditions: 220 °C, 26–29 bar (initial Ar pressure set at 5 bar), 20 mL of wastewater, 0.4 g of Pt/C catalyst, 500 rpm, 4 h.

**Fig. 9.** (a) Selectivity, (b) alkanes selectivity and (c) H₂ and alkanes yield in APR of SSW and RSW*. *Reaction conditions: 220 °C, 26–29 bar (initial Ar pressure set at 5 bar), 20 mL of wastewater, 0.4 g of Pt/C catalyst, 500 rpm, 4 h.

its high protein content, can affect the performance of the catalyst largely in comparison to other starch-based wastewater that had a lower protein concentration. Therefore, to evaluate the effect of the protein content on catalysts stability, the catalysts used in the APR of PPW and SSW were tested in a 2nd APR cycle. In the second cycle both catalysts were tested using SSW as feedstock. Fig. 10 (a) shows the TOC and COD removal obtained upon 2 successive APR cycles. As can be seen, the TOC and COD removal in the 2nd cycle was similar to the 1st one for the catalyst only used in the APR of SSW, showing non-significant loss of activity. However, the catalyst used first in the APR of PPW exhibited a much lower removal of TOC and COD in the 2nd cycle with SSW, evidencing some catalyst deactivation during the 1st cycle. Furthermore, the elemental analysis of the Pt/C catalyst used with PPW (both in the 1st and 2nd cycles) showed higher N and S contents than using SSW (Table S1).

Table 5 shows the gas volume produced, gas composition, CCgas, CCliq and CCsol upon 2 successive APR cycles for the catalysts used in the APR of SSW and PPW. The gas volume produced and the percentage of H₂ in the gas fraction slightly increased in the 2nd cycle for the catalyst only used in the APR of SSW. On the for the catalyst used with PPW in the 1st APR cycle, the percentage of H₂ that was reduced by half, remaining at only 15.7 % in the 2nd cycle with SSW. In addition, the percentage of CO₂ in the gas fraction was similar in both cycles for the catalyst only used with SSW (32.8–33.2 %), while it increased from 52.3

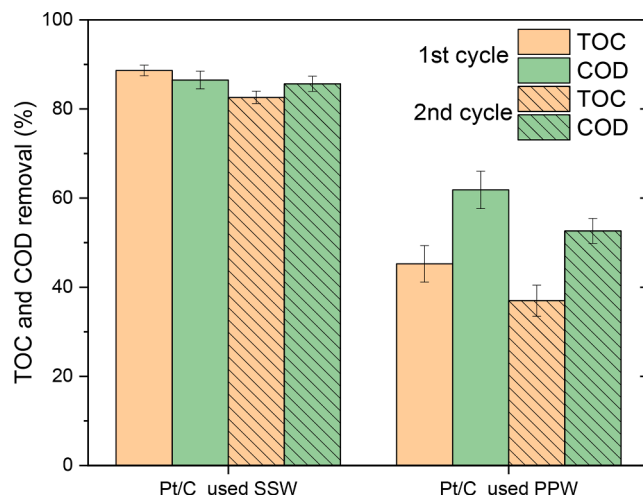
**Fig. 10.** (a) TOC and COD removal upon 2 successive APR cycles*. *Reaction conditions: 220 °C, 26–29 bar (initial Ar pressure set at 5 bar), 20 mL of wastewater, 0.4 g of Pt/C catalyst, 500 rpm, 4 h.

Table 5

Results obtained upon 2 successive APR cycles*.

Sample	Cycle (wastewater used)	Gas volume (mL)	Gas composition (% mol)					CCgas (%)	CCliq (%)	CCsol (%)
			H ₂	CO ₂	CH ₄	C ₂ H ₆	C ₃ H ₈			
Pt/C _{used} SSW	1st (SSW)	183.1 ± 5.8	60.2 ± 0.7	33.2 ± 1.6	3.3 ± 1.3	2.5 ± 0.2	0.8 ± 0.1	44.3 ± 0.3	11.4 ± 1.2	44.3 ± 0.9
	2nd (SSW)	186.8 ± 0.2	64.1 ± 0.2	32.8 ± 0.2	1.5 ± 0.1	1.2 ± 0.1	0.5 ± 0.1	48.3 ± 0.4	17.4 ± 1.4	34.3 ± 1.0
Pt/C _{used} PPW	1st (PPW)	41.9 ± 0.4	35.4 ± 0.1	52.3 ± 0.1	10.0 ± 0.1	1.7 ± 0.1	0.6 ± 0.1	17.2 ± 0.2	54.7 ± 4.1	28.0 ± 3.9
	2nd (SSW)	35.0 ± 0.1	15.7 ± 0.2	79.9 ± 0.2	2.8 ± 0.1	1.4 ± 0.1	0.3 ± 0.1	20.5 ± 0.1	63.0 ± 3.5	16.5 ± 3.4

*Reaction conditions: 220 °C, 26–29 bar (initial Ar pressure set at 5 bar), 20 mL of wastewater, 0.4 g of Pt/C catalyst, 500 rpm, 4 h.

to 79.9 % for the catalyst previously used with PPW in the first cycle. As indicated above the increase in CO₂ can reflect higher contribution of competing HTC due to loss of catalytic activity. These results are also in agreement with the elemental analysis of the Pt/C catalyst mentioned above (Table S1).

Regarding the selectivity and yields obtained, the selectivity to H₂ increased in the 2nd cycle for both catalysts due to a decreased of the selectivity to the production of alkanes (Fig. 11 (a) and (b)). On the other hand, the yield to H₂ for the catalysts used two cycles with SSW was even higher in the 2nd cycle than in the 1st, whereas for the catalyst used with PPW in the 1st cycle decreased.

4. Conclusions

The starch wastewater was subjected to aqueous phase reforming for the green hydrogen production. Successful results indicate that some biopolymers can be reformed in a one-pot process. Different Pt and Pt-based bimetallic catalysts were tested in the SSW reforming experiments to determine the most active catalyst under the reaction conditions used. Relevant TOC and COD removal values, as high as 99.1 %, were achieved for all catalysts, except in the case of PtRe/C, which showed removal values in a range similar to that of blank experiments (55.9–68.0 %), possibly due to its higher surface acidity. On the other hand, PtRu/C and Pt/C catalyst achieved the highest H₂ yield values, around 51 mmol H₂ gTOC_i⁻¹, although PtRu/C showed significantly

lower H₂ selectivity than the Pt/C catalyst (61.3 versus 77.6 %). The differences in catalytic behavior showed the importance of experimental catalyst screening, as catalyst performance cannot be predicted.

In the experiments with real wastewaters, an influence of starch source could be observed in the organic matter removal. APR of rice, sweet potato and cassava processing wastewater resulted in high TOC and COD removal values, between 70.9 and 85.4 %, comparable to the behavior of synthetic wastewaters. On the contrary, TOC and COD removal values were significantly lower for potato processing wastewater (45.3–61.8 %). Starch conversion was high, between 99 and 100 %, in all the experiments, and H₂ yield was higher at higher initial starch concentration, except in the case of potato processing wastewater, which achieved the lowest values due to its high protein content. The highest H₂ yield (28.5 mmol H₂ gTOC_i⁻¹) was reached with rice processing wastewater. This work shows the great potential of starch-based wastewater to produce H₂ through APR, since the results in this work were significantly better than those obtained with other types of wastewaters, such as brewery wastewater. In addition, it was observed that not only a high starch concentration in the wastewater is important to achieve a H₂ high yield of, but also a low content of other compounds such as proteins, which affect catalytic activity. Valorization by APR of starch wastewater with high protein content requires pre-treatment for protein removal.

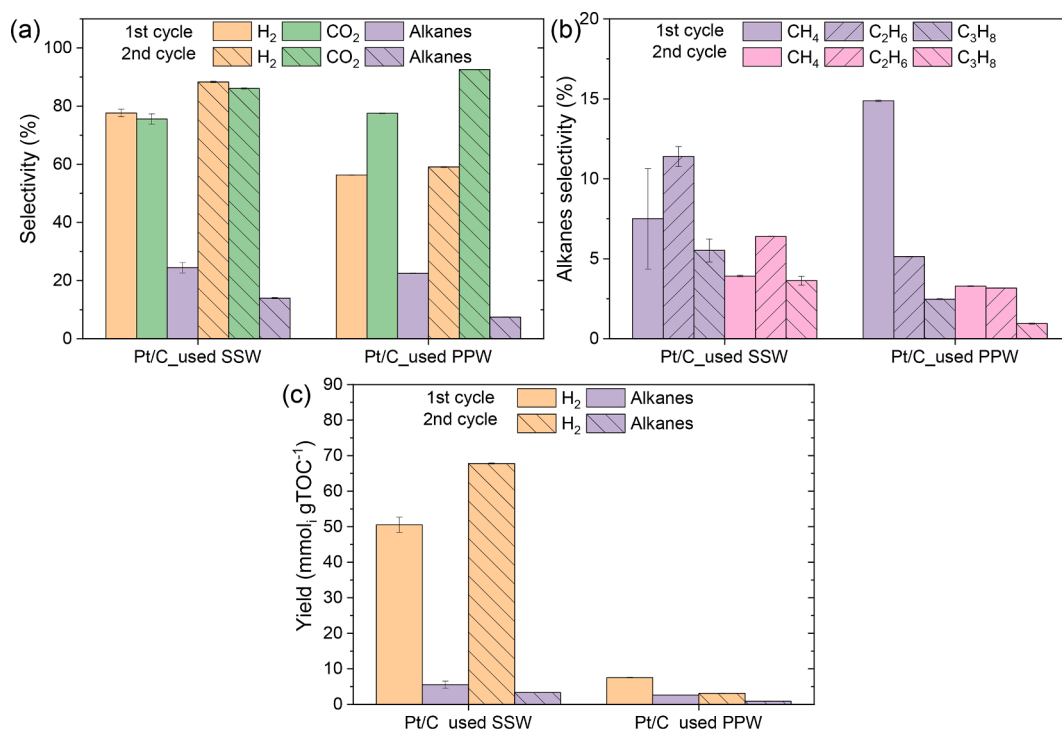


Fig. 11. (a) Selectivity, (b) alkanes selectivity and (c) H₂ and alkanes yield upon 2 successive APR cycles*. *Reaction conditions: 220 °C, 26–29 bar (initial Ar pressure set at 5 bar), 20 mL of wastewater, 0.4 g of Pt/C catalyst, 500 rpm, 4 h.

Declaration of Competing Interest

The authors declare that they have no known competing financial interests or personal relationships that could have appeared to influence the work reported in this paper.

Data availability

No data was used for the research described in the article.

Acknowledgements

Adriana S. Oliveira thanks the Ministry of Universities; The Recovery, Transformation and Resilience Plan, and the Autonomous University of Madrid for a research grant (CA1/RSUE/2021-00836).

Appendix A. Supplementary data

Supplementary data to this article can be found online at <https://doi.org/10.1016/j.cej.2023.141770>.

References

- [1] E. Commission, D.-G. for Energy, B. Breitschopf, L. Zheng, M. Plaisir, D. Kawale, J. Koornneef, Y. Melese, M. Schaaphok, J.G. Dedecca, C. Bene, O. Cerny, F. Gérard, The role of renewable H₂ import & storage to scale up the EU deployment of renewable H₂, 2022. <https://doi.org/10.2833/727785>.
- [2] A. Velazquez Abad, P.E. Dodds, Green hydrogen characterisation initiatives: definitions, standards, guarantees of origin, and challenges, *Energy Policy*. 138 (2020), 111300, <https://doi.org/10.1016/j.enpol.2020.111300>.
- [3] B. You, Y. Sun, Innovative strategies for electrocatalytic water splitting, *Acc. Chem. Res.* 51 (2018) 1571–1580, <https://doi.org/10.1021/acs.accounts.8b00002>.
- [4] D. Guban, I.K. Muritala, M. Roeb, C. Sattler, Assessment of sustainable high temperature hydrogen production technologies, *Int. J. Hydrogen Energy*. 45 (2020) 26156–26165, <https://doi.org/10.1016/j.ijhydene.2019.08.145>.
- [5] J. Qi, W. Zhang, R. Cao, Solar-to-hydrogen energy conversion based on water splitting, *Adv. Energy Mater.* 8 (2018) 1–16, <https://doi.org/10.1002/aenm.201701620>.
- [6] A. Zappi, R. Hernandez, W.E. Holmes, A review of hydrogen production from anaerobic digestion, *Int. J. Environ. Sci. Technol.* 18 (2021) 4075–4090, <https://doi.org/10.1007/s13762-020-03117-w>.
- [7] R.C. Saxena, D. Seal, S. Kumar, H.B. Goyal, Thermo-chemical routes for hydrogen rich gas from biomass: a review, *Renew. Sustain. Energy Rev.* 12 (2008) 1909–1927, <https://doi.org/10.1016/j.rser.2007.03.005>.
- [8] A. Arregi, M. Amutio, G. Lopez, J. Bilbao, M. Olazar, Evaluation of thermochemical routes for hydrogen production from biomass: a review, *Energy Convers. Manag.* 165 (2018) 696–719, <https://doi.org/10.1016/j.enconman.2018.03.089>.
- [9] A.S. Oliveira, J.A. Baeza, L. Calvo, N. Alonso-Morales, F. Heras, J.J. Rodriguez, M. A. Gilarranz, Production of hydrogen from brewery wastewater by aqueous phase reforming with Pt/C catalysts, *Appl. Catal. B Environ.* 245 (2019) 367–375, <https://doi.org/10.1016/j.apcatb.2018.12.061>.
- [10] D.A. Sladkovskiy, L.I. Godina, K.V. Semikin, E.V. Sladkovskaya, D.A. Smirnova, D. Y. Murzin, Process design and techno-economical analysis of hydrogen production by aqueous phase reforming of sorbitol, *Chem. Eng. Res. Des.* 134 (2018) 104–116, <https://doi.org/10.1016/j.cherd.2018.03.041>.
- [11] F. Aiouache, L. McAleer, Q. Gan, A.H. Al-Muhtaseb, M.N. Ahmad, Path lumping kinetic model for aqueous phase reforming of sorbitol, *Appl. Catal. A Gen.* 466 (2013) 240–255, <https://doi.org/10.1016/j.apcata.2013.06.039>.
- [12] G.-y. Chen, W.-Q. Li, H. Chen, B.-B. Yan, Progress in the aqueous-phase reforming of different biomass-derived alcohols for hydrogen production 生物质衍生醇类水相重整制氢研究进展, *J. Zhejiang Univ. Sci. A (Applied Phys. Eng.)* 16 (6) (2015) 491–506.
- [13] R.R. Davda, J.A. Dumesic, Renewable hydrogen by aqueous-phase reforming of glucose, *Chem. Commun.* 10 (2004) 36–37, <https://doi.org/10.1002/anie.200353050>.
- [14] R.R. Davda, J.W. Shabaker, G.W. Huber, R.D. Cortright, J.A. Dumesic, A review of catalytic issues and process conditions for renewable hydrogen and alkanes by aqueous-phase reforming of oxygenated hydrocarbons over supported metal catalysts, *Appl. Catal. B Environ.* 56 (2005) 171–186, <https://doi.org/10.1016/j.apcatb.2004.04.027>.
- [15] G. Pipitone, G. Zoppi, R. Pirone, S. Bensaid, A critical review on catalyst design for aqueous phase reforming, *Int. J. Hydrogen Energy*. 47 (2022) 151–180, <https://doi.org/10.1016/j.ijhydene.2021.09.206>.
- [16] P.D. Vaidya, J.A. Lopez-Sanchez, Review of hydrogen production by catalytic aqueous-phase reforming, *ChemistrySelect*. 2 (2017) 6563–6576, <https://doi.org/10.1002/slct.201700905>.
- [17] C. He, J. Zheng, K. Wang, H. Lin, J.-Y. Wang, Y. Yang, Sorption enhanced aqueous phase reforming of glycerol for hydrogen production over Pt-Ni supported on multi-walled carbon nanotubes, *Appl. Catal. B Environ.* 162 (2015) 401–411, <https://doi.org/10.1016/j.apcatb.2014.07.012>.
- [18] T. Van Haasterecht, M. Swart, K.P. De Jong, J.H. Bitter, Effect of initial nickel particle size on stability of nickel catalysts for aqueous phase reforming, *J. Energy Chem.* 25 (2016) 289–296, <https://doi.org/10.1016/j.jechem.2016.01.006>.
- [19] I. Coronado, M. Stekrova, M. Reinikainen, P. Simell, L. Lefferts, J. Lehtonen, A review of catalytic aqueous-phase reforming of oxygenated hydrocarbons derived from biorefinery water fractions, *Int. J. Hydrogen Energy*. 41 (2016) 11003–11032, <https://doi.org/10.1016/j.ijhydene.2016.05.032>.
- [20] A. Fasolini, R. Cucciniello, E. Paone, F. Mauriello, T. Tabanelli, A short overview on the hydrogen production via aqueous phase reforming (APR) of cellulose, C6–C5 sugars and polyols, *Catalysts*. 9 (2019) 917, <https://doi.org/10.3390/catal9110917>.
- [21] G. Zoppi, G. Pipitone, R. Pirone, S. Bensaid, Aqueous phase reforming process for the valorization of wastewater streams: application to different industrial scenarios, *Catal. Today*. 387 (2022) 224–236, <https://doi.org/10.1016/j.cattod.2021.06.002>.
- [22] A.S. Oliveira, A. Sarrión, J.A. Baeza, E. Diaz, L. Calvo, A.F. Mohedano, M. A. Gilarranz, Integration of hydrothermal carbonization and aqueous phase reforming for energy recovery from sewage sludge, *Chem. Eng. J.* 442 (2022), 136301, <https://doi.org/10.1016/j.cej.2022.136301>.
- [23] A. Di Fraia, E. Miliotti, A.M. Rizzo, G. Zoppi, G. Pipitone, R. Pirone, L. Rosi, D. Chiamonti, S. Bensaid, Coupling hydrothermal liquefaction and aqueous phase reforming for integrated production of biocrude and renewable H₂, *AIChE J.* (2022) 1–14, <https://doi.org/10.1002/aic.17652>.
- [24] A.S. Oliveira, T. Cordero-Lanzac, J.A. Baeza, L. Calvo, J.J. Rodriguez, M. A. Gilarranz, Continuous aqueous phase reforming of wastewater streams: a catalyst deactivation study, *Fuel*. 305 (2021), 121506, <https://doi.org/10.1016/j.fuel.2021.121506>.
- [25] R. V. Stick, S.J. Williams, Carbohydrates: The Essential Molecules of Life, 2nd Edition, Elsevier, 2009. <https://doi.org/10.1016/B978-0-240-52118-3.X0001-4>.
- [26] A. Aho, M. Alvear, J. Ahola, J. Kangas, J. Tanskanen, I. Simakova, J.L. Santos, K. Eränen, T. Salmi, D.Y. Murzin, H. Grénman, Aqueous phase reforming of birch and pine hemicellulose hydrolysates, *Bioresour. Technol.* 348 (2022) 4–10, <https://doi.org/10.1016/j.biortech.2022.126809>.
- [27] A.S. Oliveira, A. Aho, J.A. Baeza, L. Calvo, I.L. Simakova, M.A. Gilarranz, D. Y. Murzin, Enhanced H₂ production in the aqueous-phase reforming of maltose by feedstock pre-hydrogenation, *Appl. Catal. B Environ.* 281 (2021), 119469, <https://doi.org/10.1016/j.apcatb.2020.119469>.
- [28] D. Faría, A. Oliveira, J.A. Baeza, B. Saenz de Miera, L. Calvo, M.A. Gilarranz, L. Naval, Sewage treatment using Aqueous Phase Reforming for reuse purpose, *J. Water Process Eng.* 37 (2020), 101413, <https://doi.org/10.1016/j.jwpe.2020.101413>.
- [29] R. Sirohi, J. Joun, J.Y. Lee, B.S. Yu, S.J. Sim, Waste mitigation and resource recovery from food industry wastewater employing microalgae-bacterial consortium, *Bioresour. Technol.* 352 (2022), 127129, <https://doi.org/10.1016/j.biortech.2022.127129>.
- [30] J.A. Zazo, J.A. Casas, A.F. Mohedano, J.J. Rodríguez, Catalytic wet peroxide oxidation of phenol with a Fe/active carbon catalyst, *Appl. Catal. B Environ.* 65 (2006) 261–268, <https://doi.org/10.1016/j.apcatb.2006.02.008>.
- [31] S. Mukerjee, S. Srinivasan, M.P. Soriaga, J. McBrean, Role of structural and electronic properties of Pt and Pt Alloys on electrocatalysis of oxygen reduction: an in situ XANES and EXAFS investigation, *J. Electrochem. Soc.* 142 (5) (1995) 1409–1422.
- [32] V.W.S. Lam, A. Alfantazi, E.L. Gyenge, The effect of catalyst support on the performance of PtRu in direct borohydride fuel cell anodes, *J. Appl. Electrochem.* 39 (2009) 1763–1770, <https://doi.org/10.1007/s10800-009-9875-5>.
- [33] Y.-T. Hung, H. Salman, H. Lo, A. Awad, Waste Treatment in the Food Processing Industry, 1st ed., CRC Press, 2005. <https://doi.org/10.1201/9781420037128>.
- [34] B. Kaya, S. Irmak, A. Hasanoglu, O. Erbatır, Developing Pt based bimetallic and trimetallic carbon supported catalysts for aqueous-phase reforming of biomass-derived compounds, *Int. J. Hydrogen Energy*. 40 (2015) 3849–3858, <https://doi.org/10.1016/j.ijhydene.2015.01.131>.
- [35] A. Larimi, F. Khorasheh, Renewable hydrogen production over Pt/Al₂O₃ nano-catalysts: effect of M-promoting (M=Pt, Rh, Re, Ru, Ir, Cr), *Int. J. Hydrogen Energy*. 44 (2019) 8243–8251, <https://doi.org/10.1016/j.ijhydene.2019.01.251>.
- [36] L.I. Godina, A.V. Kirilin, A.V. Tokarev, I.L. Simakova, D.Y. Murzin, Sibunit-supported mono- and bimetallic catalysts used in aqueous-phase reforming of xylitol, *Ind. Eng. Chem. Res.* 57 (2018) 2050–2067, <https://doi.org/10.1021/acs.iecr.7b04937>.
- [37] A.V. Kirilin, A.V. Tokarev, E.V. Murzina, L.M. Kustov, J.P. Mikkola, D.Y. Murzin, Reaction products and transformations of intermediates in the aqueous-phase reforming of sorbitol, *ChemSusChem*. 3 (2010) 708–718, <https://doi.org/10.1002/cssc.200900254>.
- [38] D.J.M. De Vlieger, B.L. Mojet, L. Lefferts, K. Seshan, Aqueous Phase Reforming of ethylene glycol - Role of intermediates in catalyst performance, *J. Catal.* 292 (2012) 239–245, <https://doi.org/10.1016/j.jcat.2012.05.019>.
- [39] E.L. Kunkes, R.R. Soares, D.A. Simonetti, J.A. Dumesic, An integrated catalytic approach for the production of hydrogen by glycerol reforming coupled with water-gas shift, *Appl. Catal. B Environ.* 90 (2009) 693–698, <https://doi.org/10.1016/j.apcatb.2009.04.032>.
- [40] M.F. Neira D'Angelo, V. Ordonsky, J. Van Der Schaaf, J.C. Schouten, T.A. Nijhuis, Continuous hydrogen stripping during aqueous phase reforming of sorbitol in a washcoated microchannel reactor with a Pt-Ru bimetallic catalyst, *Int. J. Hydrogen*

- Energy. 39 (2014) 18069–18076, <https://doi.org/10.1016/j.ijhydene.2014.02.167>.
- [41] J. Liang, Y. Liu, J. Zhang, Effect of Solution pH on the Carbon Microsphere Synthesized by Hydrothermal Carbonization, *Procedia, Environ. Sci.* 11 (2011) 1322–1327, <https://doi.org/10.1016/j.proenv.2011.12.198>.
- [42] A. Funke, F. Ziegler, Hydrothermal carbonization of biomass: a summary and discussion of chemical mechanisms for process engineering, *Biofuels Bioprod. Biorefining.* 4 (2010) 160–177, <https://doi.org/10.1002/bbb.198>.
- [43] R.R. Davda, J.W. Shabaker, G.W. Huber, R.D. Cortright, J.A. Dumesic, Aqueous-phase reforming of ethylene glycol on silica-supported metal catalysts, *Appl. Catal. B Environ.* 43 (2003) 13–26, [https://doi.org/10.1016/S0926-3373\(02\)00277-1](https://doi.org/10.1016/S0926-3373(02)00277-1).
- [44] M.F. Neira D'Angelo, V. Ordonsky, J. van der Schaaf, J.C. Schouten, T.A. Nijhuis, Selective Production of Methane from Aqueous Biocarbhydrate Streams over a Mixture of Platinum and Ruthenium Catalysts, *ChemSusChem.* 7 (2014) 627–630, <https://doi.org/10.1002/cssc.201300828>.
- [45] A. Ciftci, D.A.J.M. Ligthart, E.J.M. Hensen, Aqueous phase reforming of glycerol over Re-promoted Pt and Rh catalysts, *Green Chem.* 16 (2014) 853–863, <https://doi.org/10.1039/C3GC42046A>.
- [46] A. Ciftci, D.A.J.M. Ligthart, A.O. Sen, A.J.F. Van Hoof, H. Friedrich, E.J.M. Hensen, Pt-Re synergy in aqueous-phase reforming of glycerol and the water-gas shift reaction, *J. Catal.* 311 (2014) 88–101, <https://doi.org/10.1016/j.jcat.2013.11.011>.
- [47] T. Soták, M. Hronec, I. Vávra, E. Dobročka, Sputtering processed tungsten catalysts for aqueous phase reforming of cellulose, *Int. J. Hydrogen Energy.* 41 (2016) 21936–21944, <https://doi.org/10.1016/j.ijhydene.2016.08.183>.
- [48] A.S. Oliveira, J.A. Baeza, B. Saenz de Miera, L. Calvo, J.J. Rodriguez, M. A. Gilarranz, Aqueous phase reforming coupled to catalytic wet air oxidation for the removal and valorisation of phenolic compounds in wastewater, *J. Environ. Manage.* 274 (2020), 111199, <https://doi.org/10.1016/j.jenvman.2020.111199>.